

Article

Microwave-Assisted Catalytic Conversion of 5-HMF for Biofuel Additives by Molybdophosphoric Acid Encapsulated KCC-1

Srinivasan Vinju Vasudevan ¹, Jin Cai ¹, Junming Xu ², Hongjian Lin ³, Hongliang Wang ⁴ and Quan Bu ^{1,*}

¹ Key Laboratory of Modern Agricultural Equipment and Technology, Ministry of Education, Jiangsu University, Zhenjiang 212013, China

² Institute of Chemical Industry of Forest Products, Chinese Academy of Forestry, Key Laboratory of Biomass Energy and Material, Jiangsu Province, National Engineering Laboratory for Biomass Chemical Utilization, Nanjing 210042, China

³ College of Biosystems Engineering and Food Science, Zhejiang University, Hangzhou 310058, China

⁴ College of Agronomy and Biotechnology/Center of Biomass Engineering, China Agricultural University, Beijing 100193, China

* Correspondence: qbu@ujs.edu.cn; Tel.: +86-511-88797338

Abstract: In this work, the microwave-assisted reaction of 5-hydroxymethylfurfural (5-HMF) into valuable ether and acylated production formation was investigated with the help of molybdophosphoric acid encapsulated dendritic fibrous silica (KCC-1) as a catalyst. XRD, N₂ adsorption-desorption, SEM, FT-IR, NH₃-TPD, and TEM were used to analyze the physicochemical and structural properties of the synthesized catalysts. The microwave etherification of 5-HMF with ethanol was tested using synthesized catalysts. The effects of the reaction temperature, reaction time, catalytic amount, and microwave power were investigated. The resulting MPA-KCC-1 and IMPA-KCC-1 catalysts demonstrated excellent activity for the etherification of 5-HMF with ethanol, producing 5-(hydroxymethyl) furfural diethyl acetal (HMFDEA) and 5-(ethoxymethyl)furfural diethyl acetal (EMFDEA) products selectively. The significant advantages of the work are the selective production of EMFDEA at 82%, the catalyst can be easily removed via filtration, and the catalyst activity remains nearly intact even after five reaction cycles.

Keywords: biomass; acetylation; 5-HMF; etherification; heteropolyacid; fibrous silica



Citation: Vasudevan, S.V.; Cai, J.; Xu, J.; Lin, H.; Wang, H.; Bu, Q. Microwave-Assisted Catalytic Conversion of 5-HMF for Biofuel Additives by Molybdophosphoric Acid Encapsulated KCC-1. *Catalysts* **2023**, *13*, 969. <https://doi.org/10.3390/catal13060969>

Academic Editor:
Federica Menegazzo

Received: 10 May 2023
Revised: 27 May 2023
Accepted: 31 May 2023
Published: 2 June 2023



Copyright: © 2023 by the authors. Licensee MDPI, Basel, Switzerland. This article is an open access article distributed under the terms and conditions of the Creative Commons Attribution (CC BY) license (<https://creativecommons.org/licenses/by/4.0/>).

1. Introduction

Global warming is consistently growing due to the rapid consumption of fossil fuels, which creates a situation for researchers to find suitable alternative fuels. Biomass is considered one of the renewable energy sources and has received great attention among researchers, being sustainable to the environment and helping to reduce carbon footprints [1–4]. Moreover, biomass is a potential source for producing value-added chemicals, sustainable fuels, and renewable catalytic materials [5–8]. The organic compound 5-hydroxymethylfurfural (5-HMF) is derived from biomass carbohydrates, such as glucose and fructose, through acid-catalyzed dehydration. It is a versatile platform chemical with a wide range of applications, including as a fuel additive and as a precursor for the production of various chemicals and materials [8–10].

The 5-HMF can be upgraded through aldol condensation, esterification, etherification, amination, reduction, and oxidation [8,11]. The etherification or acetylation of 5-HMF are classes of reaction for biofuel additive synthesis with a high energy density, and they are also interesting for fundamental research [12,13]. Typically, the etherification of 5-HMF has been performed with ethanol and other lower-carbon alcohols in the presence of solid acid catalysts. Most of the solid acid catalysts have been reported for 5-EMF or 5-alkoxy methyl furfural synthesis from 5-HMF, including ambertlyst-15 [14,15], Al-MCM-41 [13,16],

H-BEA [17], and a metal–organic framework [18]. Recently, Guo et al. reported the production of 5-(hydroxymethyl)-2-(dimethoxymethyl) furan (HDMF), 5-(methoxymethyl)-2-furaldehyde, and 2-(dimethoxymethyl)-5-(methoxymethyl) furan (DMMF) by the reaction of methanol with 5-HMF when using $\text{SiO}_2\text{--HNO}_3$ as a catalyst and silica-supported nitric acid as a solid acid catalyst, effectively synthesizing acetylated products [19]. Therefore, the properties of the catalyst and the reaction conditions determine the distribution of the reaction products in 5-HMF conversion. Overall, the development of effective and sustainable processes for the production of 5-HMF derivatives has great potential to contribute to the development of a more sustainable and environmentally friendly chemical and energy industry. However, improved and sustainable manufacturing processes for 5-HMF derivatives synthesis are still required. Therefore, researchers are actively exploring new catalysts and optimizing the reaction conditions to improve the efficiency, selectivity, and sustainability of 5-HMF conversion processes.

Polyoxometalates, especially with Keggin structured molybdophosphoric acid (MPA), have thermal stability and strong Brønsted acidity due to their metal–oxygen framework. Moreover, molybdophosphoric acid poses a lower environmental hazard compared with other inorganic acids and it is used as an ideal catalyst for many fine chemical syntheses and biomass conversion reactions [20,21]. However, MPAs are difficult to separate from the reaction mixture since they are well-soluble in polar and water-based solvents. To boost their stability, efficiency, and heterogeneity, they can be supported on solid matrices such as silica [22], carbon [23], MOF [24], and zeolite [25]. Designing MPA-immobilized heterogeneous acid catalysts for esterification processes has been investigated using a variety of solid supports, including mesoporous MCM-41 silica [26], zirconia [27], activated carbonaceous materials, and alumina [28]. The mesoporous silica materials have a high surface area, pore volume, and pore size, along with sufficiently accessible diffusion channels linked to micro-to-mesoporous structures, which are distinctive advantages [29]. Modifying the surface of mesoporous silica with MPA groups has received much attention due to their specific application in the field of catalysis. Although molybdophosphorics have been extensively studied as catalysts for different reactions, their specific application in the etherification and acylation of 5-HMF is relatively limited. Specially, the encapsulation of MPA molecules in dendritic fibrous silica material can create effective solid acid catalysts with improved catalytic properties for 5-HMF etherification.

It is known that microwave-assisted heating has a great number of advantages compared with conventional heating, since the heat is generated via molecule friction, so the heat is passed on from the inside to the outside of the sample, which contributes to a smaller amount of heat loss and energy efficiency due to fast and selective heating [30]. Consequently, it can promote the chemical reaction and improve the product's quality; recently, microwave-assisted heating technologies such as pyrolysis, hydrothermal liquefaction, and gasification have been widely utilized in biomass conversion for biofuel and chemicals [31]. However, most of the 5-HMF etherification has been carried out under conventional heating but has not been studied so far in microwave conditions. In this work, the synthesized MPA encapsulated KCC-1 was taken as a catalyst for 5-HMF etherification with ethanol under microwave conditions and the catalytic activity studied for different temperatures, catalyst loading, times, and microwaves. The valuable intermediates of 5-HMF acetylated and ether products in 5-HMF with ethanol reactions would be useful fuel additives in biorefinery processes.

2. Results and Discussions

2.1. Characterization Analysis

Figure 1 shows the XRD patterns of the unmodified pure KCC-1 and MPA-modified KCC-1 catalysts. The optimized amount of MPA was 20 wt.% from the reported literature and the same amount was taken to encapsulate in the KCC-1 silica material. The morphological structure of the KCC-1 silica materials collapsed if the increase in the encapsulation of MPA wt.% was more than 20 with KCC-1. The 20 wt.% impregnated on KCC-1 was synthesized to evaluate the catalytic activity with the encapsulated one [32,33]. All of the prepared

materials showed a large peak at 2θ degrees at 23° in the X-ray diffraction, indicating the silica's characteristic amorphous nature (Figure 1). In addition, the absence of MPA or its crystalline decomposition diffraction lines within the MPA-KCC-1 catalyst implied that the MPA molecules were distributed evenly in the silica matrix with Keggin units [34]. The primary XRD lines in the IMPA-KCC-1 were at 2θ , 13.8° , 23.5° , 26.3° , 27.2° , 34° , and 39.2° ; these peaks are aligned with the crystalline peaks of the pure MPA molecule. These peaks are typically assigned to cubic Keggin-type structures (the black color diffraction pattern in Figure 1). Due to the impregnation process, the intensity of IMPA was seen to be smaller than that of pure KCC-1 and MPA-KCC-1.

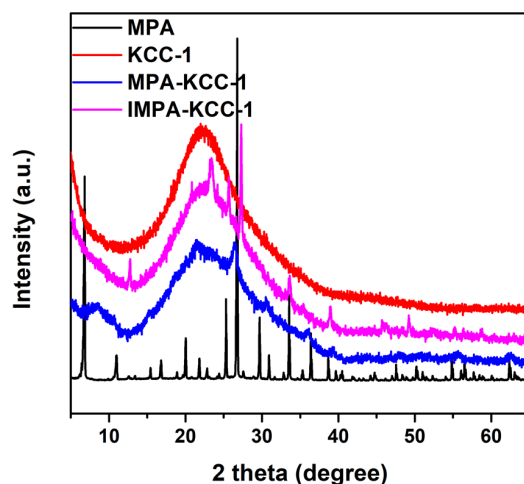


Figure 1. XRD spectra of KCC-1 catalysts.

The FT-IR spectra of the KCC-1 and MPA encapsulated and impregnated KCC-1 are shown in Figure 2. The broad peak at 3100 to 3600 cm^{-1} was assigned to the water molecules absorbed on the surface of the silica KCC-1. After the encapsulation and impregnation of MPA molecules with KCC-1 silica support, the broad peak was reduced due to the reduction of the absorbed water molecules or the interaction of $-\text{OH}$ groups with loaded MPA molecules. The heteropoly acids of the MPA molecule bonds are generally located at 1060 , 970 , 875 , and 760 cm^{-1} , corresponding to the stretching vibration of $\nu(\text{P-Oa})$, $\nu(\text{M-Od})$, $\nu(\text{M-Ob-M})$, and $\nu(\text{M-Oc-M})$ and also confirm the Keggin formations (M represents the Mo metal ions) [35]. Notably, most of the bands of the heteropoly anions overlapped with the SiO_2 peaks and create difficulties in distinguishing the peaks between the heteropoly anions and SiO_2 .

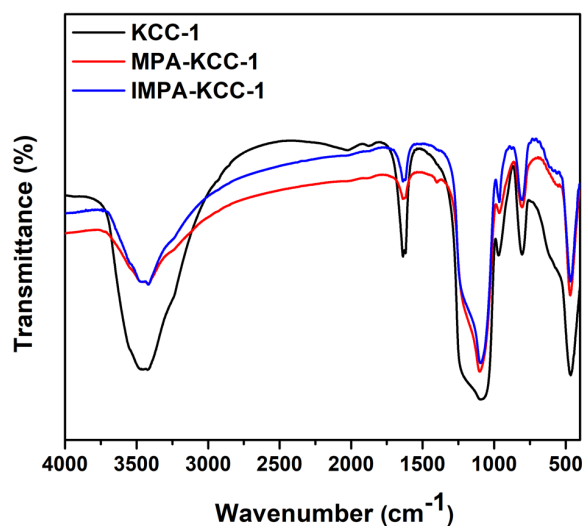


Figure 2. The FT-IR spectra of the KCC-1 catalysts.

Figure 3a,b depict the N₂ sorption isotherms and BJH pore size distribution of the KCC-1, MPA-KCC-1, and IMPA-KCC-1 catalysts, and Table 1 provides the associated textural properties. The observed Type IV isotherms with H3 hysteresis loops in all synthesized materials can specify the mesoporous nature of those materials and can also confirm the formation of the mesoporous structures with large pores [36]. KCC-1, MPA-KCC-1, and IMPA-KCC-1 each had a surface area of 523, 320, and 380 m²/g, respectively (Table 1). In Figure 3b, the BJH pore size distribution (Figure 3b) adsorbed the volume in the range of 0.4 to 0.95 P/P₀ and was observed in all the catalysts, which confirms the presence of a large pore size distribution. The encapsulation strategy decreased the BET surface of MPA-KCC-1, (320 m²/g) and pore volume (0.65 cm³/g).

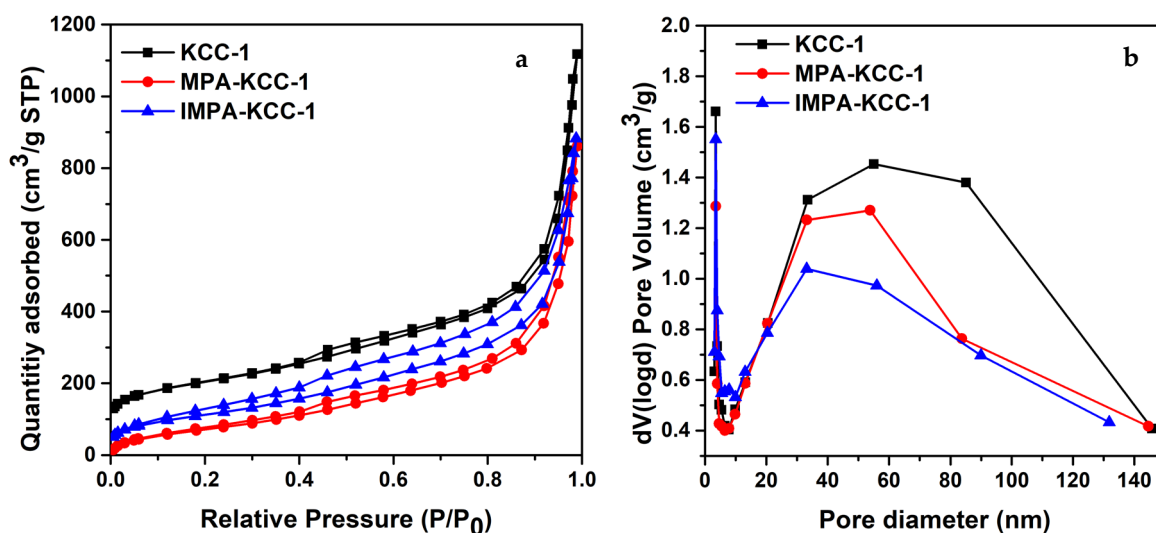


Figure 3. (a) N₂ sorption isotherms of KCC-1, MPA encapsulated and impregnated catalysts, and (b) their corresponding BJH pore size distribution.

Table 1. The mesoporosity and acidity of the KCC-1, MPA-KCC-1, and IMPA-KCC-1.

Catalyst	S _{BET} ^a (m ² /g)	V _{tp} ^b (cm ³ /g)	d _{p, BJH} ^c (nm)	Total Acidity ^d mmol NH ₃ /g
KCC-1	523	1.63	13	0.022
MPA-KCC-1	320	0.65	14	0.251
IMPA-KCC-1	380	1.20	13	0.385

^a Specific surface area, ^b total pore volume, ^c average pore diameter, ^d NH₃-TPD analysis.

The prepared samples' total acidity was evaluated using NH₃-TPD, and their desorbed ammonia profiles are displayed in Figure 4. The total acidity of the pure siliceous KCC-1 was 0.022 mmol/NH₃, which is negligible with the comparison of the total acidity of the MPA-KCC-1 and IMPA-KCC-1 catalysts (the acidic amounts are displayed in Table 1). In the NH₃-TPD profile, the weak and moderate acidic sites of the MPA-KCC-1 and IMPA-KCC-1 can be observed at 80 to 150 °C and at 300 to 450 °C. The acidity of the IMPA-KCC-1 catalyst appears to be high, which is due to the impregnation method, which accommodated more heteropoly anions in the silica matrix as well as on the material's surface, resulting in a high acidic strength. The observed total acid value of the MPA-KCC-1 catalyst was considerably lower, indicating that its heteropoly anion was lost during the catalyst wash after synthesis [33].

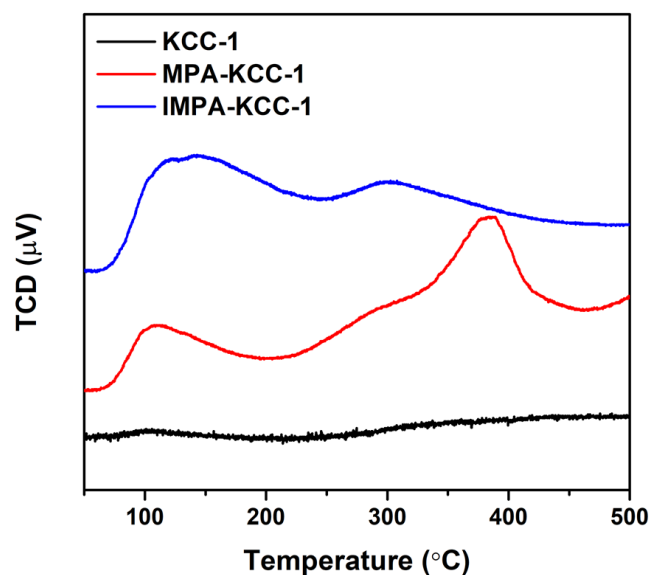


Figure 4. The TPD-NH₃ profile of KCC-1 catalysts.

The morphology of the synthesized catalysts was evaluated using SEM and TEM techniques; the related images are presented in Figures 5 and 6, respectively. Both the SEM (Figure 5a) and TEM (Figure 6a) images of unmodified KCC-1 show the well-preserved dendritic fibrous structure. The spherical morphology can be preserved during the MPA encapsulation strategy in KCC-1, allowing the MPA molecules to be filled evenly within the fibrous natured pores that can be observed in the MPA-KCC-1 SEM image (Figure 5b) [33]. Furthermore, during synthesis, MPA is encapsulated in silica, transforming the morphology of the fibrous structure into a mesoporous sphere-shaped structure with the consistent distribution of pore sizes that can be observed in the MPA-KCC-1 TEM image (Figure 6b). Due to the accommodation of MPA molecules on the surface of the material, the fibrous-natured tiny pores are covered, generating homogeneous mesopores (12 nm) with a dendritic spherical structure. The average particle size of the KCC-1 and MPA-KCC-1 is $0.4 \pm 0.05 \mu\text{m}$ and 0.38 ± 0.05 , respectively (calculated using ImageJ software). As a result, the structure of the material and particle size is unaffected by the encapsulation technique [32]. The impregnation procedure had no impact on the morphology of the KCC-1 (Figure 6c) by the impregnation process, which can be observed in the TEM image of the IMPA-KCC-1. The impregnated KCC-1 and encapsulated MPA on KCC-1 catalysts were comprehensively characterized, and then its catalytic activity for the 5-HMF etherification with ethanol was assessed.

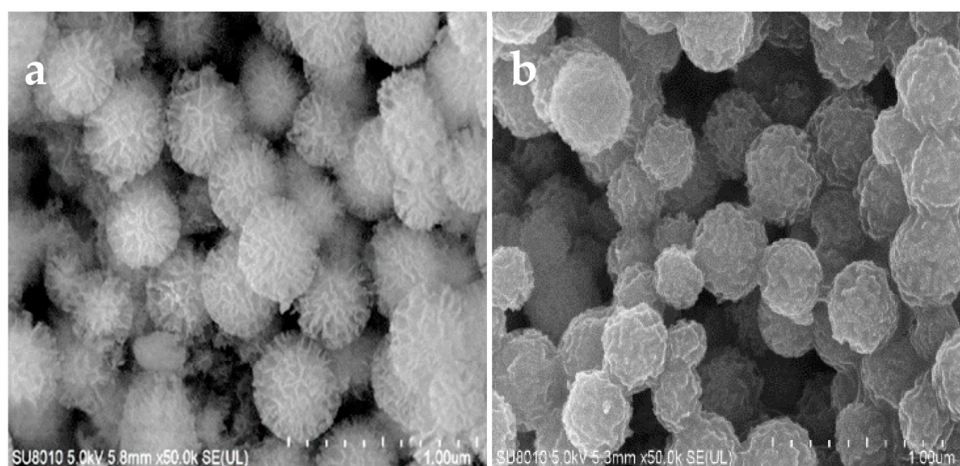


Figure 5. SEM pictures of (a) KCC-1 and (b) MPA-KCC-1.

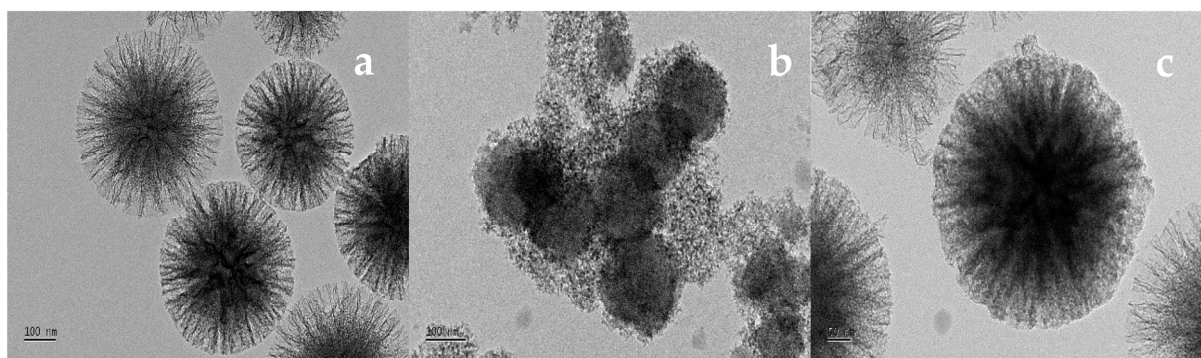


Figure 6. TEM pictures of (a) pure KCC-1, (b) MPA-KCC-1, and (c) IMPA-KCC-1.

2.2. Catalytic Activity Study on HMF Etherification and Acylation with Ethanol

The prepared MPA encapsulated and impregnated KCC-1 catalysts were tested in the microwave etherification of 5-HMF with ethanol. Initially, the MPA-KCC-1 and IMPA-KCC-1 catalytic activities were evaluated for the 5-HMF etherification with ethanol at different temperatures for 30 min; the subsequent results are shown in Figure 7. The main products were 5-(hydroxymethyl) furfural diethyl acetal (HMFDEA), 5-(ethoxymethyl)furfural diethyl acetal (EMFDEA), and minor amounts of ethyl levulinate (EL) formations were noticed. In the temperature study, the 5-HMF conversion was increased until 120 °C, then dropped in at 140 °C due to the reverse reaction of HMFDEA to 5-HMF, where the EMFDEA and ethyl levulinate (EL) selectivity were increased [37]. The HMFDEA selectivity was high at a lower temperature of 80 °C and as the temperature increased, the selectivity of HMFDEA was reduced, while the EMFDEA selectivity increased gradually to 71% at 120 °C. Further, at a higher temperature of 140 °C, the EMFDEA slightly decreased instead of the EL selectivity increasing. The temperature study reveals that a high temperature favors more EL product formation. The maximum conversion of 5-HMF and EMFDEA selectivity was obtained at 120 °C and the temperature was considered the optimum for other parameter analysis. The IMPA-KCC-1 catalyst showed a higher conversion and selectivity due to its high total acidity (0.385 mmol NH₃/g, Table 1). The surface area of both the MPA-KCC-1 and IMPA-KCC-1 catalysts was almost the same, which seemed to have no impact on the catalysis. Here, the acidity of the catalyst and the temperature of the reaction play an important role. Even though the acidity of the IMPA-KCC-1 is higher than MPA-KCC-1, it was not considered for further studies because larger amounts of heteropoly anions were leached during the reaction, which was confirmed through ICP-OES analysis of the reacted solution. In our previous study, we observed the same effect for tungstophosphoric acid encapsulated KCC-1 silica for carbohydrates to 5-HMF conversion in a microwave assisted reaction condition [32]. The catalytic activity of pure molybtophosphoric acid was evaluated in 5-HMF with ethanol at 120 °C for 30 min with a microwave power of 100 W. The 5-HMF conversion was 100% but the total yield of products was 40 to 42%, instead of more humin products being observed. Due to the high acidity of the molybtophosphoric acid, more humin products were formed compared with heterogeneous MPA-KCC-1 and IMPA-KCC-1.

To compare the effect of microwave heating, we evaluated 5-HMF etherification with ethanol in conventional heating using an oil bath with a controlled temperature at 120 °C in an autoclave for 30 and 60 min, with the corresponding results shown in Figure 8. The autoclave was kept in the oil bath after reaching the desired temperature. After 30 or 60 min the autoclave was cooled in cold water immediately. The 5-HMF conversion was 59% and the selectivity of HMFDEA, EMFDEA, and EL was 33%, 61%, and 6%, respectively, for 30 min. However, the conversion was 65% after a 60 min reaction and the EL selectivity increased to 20%. It seems that conventional heating also favors the 5-HMF conversion with a longer time compared with microwave heating. As the time increased, there was noted the formation of humin or charred products.

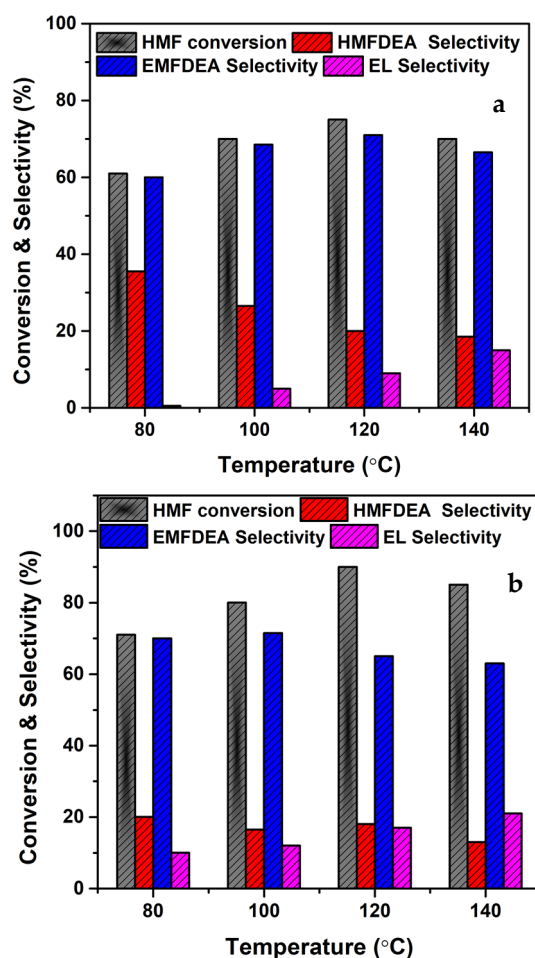


Figure 7. Different temperature studies of the modified (a) MPA-KCC-1 and (b) IMPA-KCC-1 catalysts.

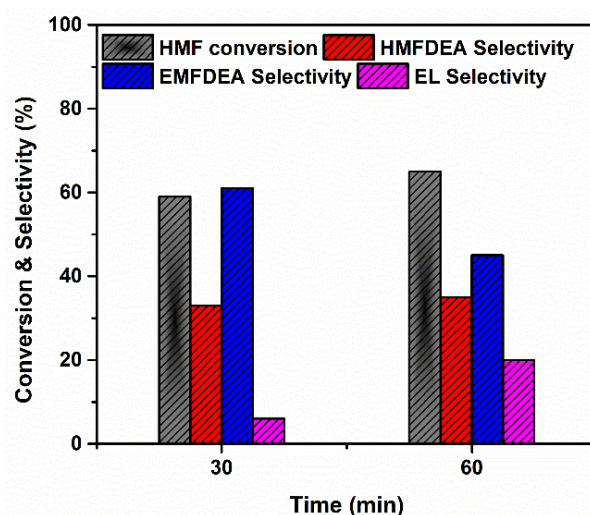


Figure 8. Activity of MPA-KCC-1 at conventional heating.

Reaction conditions: time 30 min, microwave power 100 W, ethanol 5 mL, 25 mg catalyst, 1 mmol of HMF.

Reaction conditions: temperature 120 °C, ethanol 5 mL, 25 mg catalyst, 1 mmol of 5-HMF.

Reaction conditions: temperature 120 °C, microwave power 100 W, ethanol 5 mL, 25 mg catalyst, 1 mmol of HMF.

The effect of time on the 5-HMF conversion and the corresponding selectivity was evaluated at 120 °C; the results are shown in Figure 9. The 5-HMF conversion was increased

as the time increased and the selective products of HMFDEA and EMFDEA were also increased. After 30 min, the 5-HMF conversion was decreased due to the reverse reaction of HMFDEA to 5-HMF. The maximum conversion of 75% 5-HMF with 20%, 71%, and 9% selectivity of HMFDEA, EMFDEA, and EL were formed, respectively, at 30 min. Further, the effect of the MPA-KCC-1 catalyst was studied at the different catalytic amounts at the optimum temperature of 120 °C; the results are displayed in Figure 10. The conversion of 5-HMF was 68%, 71%, and 82% for the catalytic amounts of 12.5, 25, and 37.5 mg of MPA-KCC-1, respectively. It reveals that as the catalytic amount increased, the selectivity of HMFDEA reduced from 42% to 12%, whereas the EMFDEA selectivity rose from 58% to 82%. These results suggest that an increase in catalytic amounts improves the EMFDEA selectivity due to more availability of acidic sites. In addition, the efficiency of microwave power was analyzed with varying microwave power ranges from 60 W to 100 W for the MPA-KCC-1 catalyst; the results are shown in Figure 11. The higher catalytic amount (37.5 mg) of MPA-KCC-1 was taken for different microwave power analyses and the reaction was carried out at 120 °C as the optimum temperature. It seems the different microwave powers had no great influence on the conversion of 5-HMF and the selectivity.

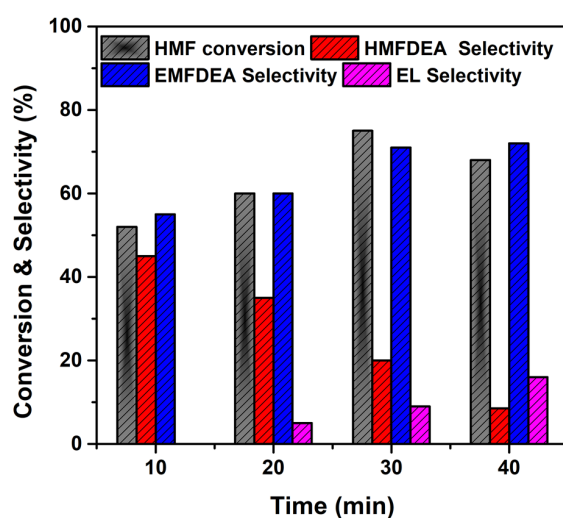


Figure 9. The catalytic activity of MPA-KCC-1 catalysts at different time intervals.

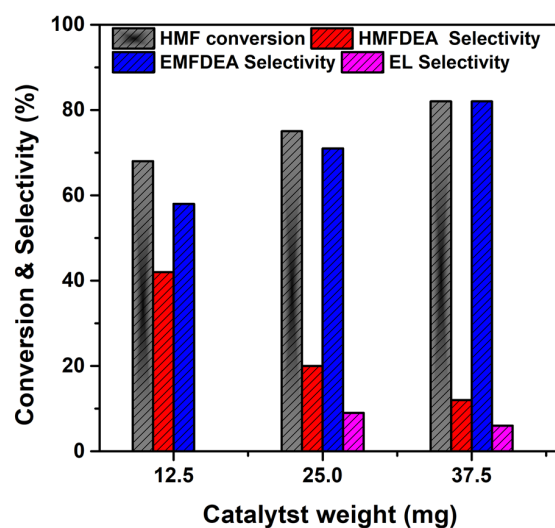


Figure 10. The effect of catalytic amounts of MPA-KCC-1.

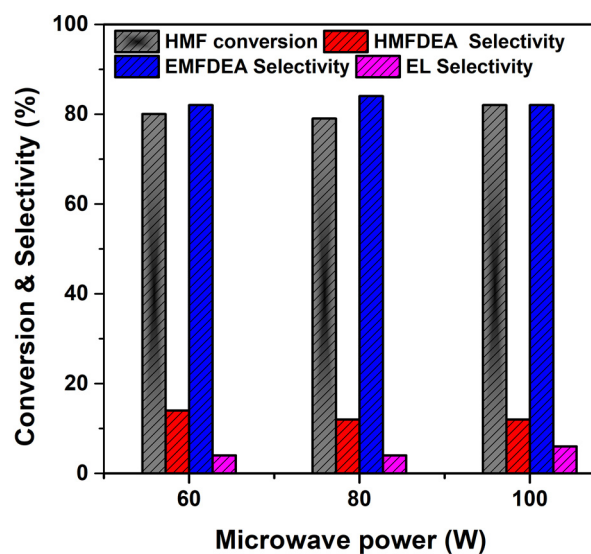


Figure 11. The effect of microwave power of MPA-KCC-1.

Reaction conditions: temperature 120 °C, time 30 min, microwave power 100 W, ethanol 5 mL, 1 mmol of HMF.

Reaction conditions: temperature 120 °C, time 30 min, ethanol 5 mL, 37.5 mg catalyst, 1 mmol of HMF.

The reusability of heterogeneous catalysts is an important industrial characteristic for evaluating the prepared catalyst's long-term catalytic performance. As a result, the reusability was further tested using five catalytic recycling experiments. The recycled experiment was conducted at an optimum parameter of 120 °C, 30 min, 100 W, 5 mL ethanol, and 37.5 mg catalyst with 1 mmol of 5-HMF. The 5-HMF conversion (82 to 75%) and the selectivity were gradually reduced in each cycle, but not too much. For reusability, the MPA-KCC-1 catalyst was filtered using 0.45-micron filter paper. The filtered catalyst was thoroughly washed three times (5 mL each time) with 70% ethanol and dried in an oven at 120 °C for 3 h, and tested for the next cycle. The recycled results are shown in Table 2. After the fifth cycle, the recovered catalyst was analyzed with ICP-OES to check the metal quantity and resulting in 5 to 6% reduced metal concentrations compared with the fresh catalyst. It is due to the metal loss in each cycle during the washing process. The recyclability of the catalyst revealed its superiority as a solid acid catalyst for potential acetylated and etherification reactions. Most researchers have reported the formation of 5-ethoxymethylfurfural (5-EMF) as a major ether product during the reaction of 5-HMF with ethanol [38]. However, in this work, we obtained acylated HMFDEA as a minor and etherified EMFDEA as a major product that would affect the acidic sites of MPA catalysts. Therefore, we generally say that the properties of the catalyst, the reaction conditions, and the acidic sites of the catalytic materials determine the distribution of the reaction products in the 5-HMF conversion.

Table 2. The reusability test of MPA-KCC-1 catalyst.

No. of Cycles	5-HMF Conversion (%) ^a	Selectivity ^b (%)		
		HMFDEA	EMFDEA	EL
1	82	13	82	5
2	80	12	84	4
3	79	10	83	7
4	73	14	81	3
5	75	12	82	6

Reaction conditions: temperature 120 °C, time 30 min, microwave power 100 W, ethanol 5 mL, 1 mmol of 5-HMF.
^a The standard deviation of each cycle conversion is ± 2.5 . ^b The standard deviation in the selectivity of each cycle is ± 2.5 .

3. Experimental

3.1. Chemicals

The carbohydrate derivatives of fructose, glucose, and cellulose substrates, and the solvents dimethyl sulphoxide (DMSO), ethanol, tetrahydrofuran (THF), methyl isobutyl ketone (MIBK), n-pentanol, p-xylene, and cyclohexanol were of analytical grade and obtained from Aladdin, Shanghai, China. The tetraethyl orthosilicate (TEOS, 98%) and molybdophosphoric acid (99%), and cetyltrimethylammonium bromide (CTAB, 99%) and urea (99%) were purchased from Sigma-Aldrich (Shanghai, China). All the chemicals and reagents were utilized in the materials synthesis and catalytic reactions as received.

3.2. Synthesis Procedure of MPA Encapsulated KCC-1

In a 250 mL beaker, 0.0027 mol of cetyltrimethylammonium bromide (CTAB) and 0.01 mol of urea with 100 mL of deionized water were mixed and stirred until the CTAB was completely dissolved. In another 500 mL beaker, a mixed solution of 0.1 mol TEOS and 100 mL p-xylene was stirred for 30 min, then drop by drop, the urea and CTAB mixed solutions were added over 30 min. The mixture of TEOS, p-xylene, CTAB, and urea was stirred for another 25 min with the slow addition of 10 mL of n-pentanol while stirring. The entire solution mixture was exchanged into a 500 mL round-bottom flask. The reaction solution was stirred for 60 min at room temperature. Then the reaction solution was kept in an oil bath and refluxed at 120 °C for 5 h. Next, 1.25 g of MPA solution (20 wt%) was added during reflux and further stirred up for 2 h. After cooling to room temperature, 100 mL of ethanol was added, and the precipitated silica material was filtered using a vacuum with deionized water washing. The filtered product was dried at 100 °C for 12 h and afterward calcined at 450 °C in a tubular furnace with an air atmosphere at a rate of 5 °C min⁻¹ and the calcined material was labeled as MPA-KCC-1. The pure KCC-1 material was synthesized using the same experimental procedure without MPA.

In addition, KCC1 impregnated with 20 wt% MPA was synthesized to compare the activity with that of encapsulated MPA-KCC-1. In a typical synthesis, 0.2 g of MPA was taken in 10 mL of deionized water and mixed with 1 g of KCC-1 in a small 100 mL beaker and stirred up for 20 h, then again heated at 100 °C until dried and kept in calcination at 450 °C in a tubular furnace with an air atmosphere for 10 h at a rate of 5 °C min⁻¹. After calcination, the obtained material was labeled as IMPA-KCC-1.

3.3. Characterizations

High-angle X-ray diffraction (XRD) of pure KCC-1, MPA-KCC-1, and IMPA-KCC-1 were recorded on a Rigaku D/max-2400 apparatus (Qingdao, China) with a step of 0.01° using Cu-K radiation as the X-ray source. The texture parameters of the samples were analyzed by nitrogen physisorption measurements using a Micromeritics ASAP 2020 (Norcross, GA, USA) porosimeter at a temperature of liquid nitrogen. All the synthesized materials were degassed at 250 °C for 5 h before analysis. Brunauer–Emmett–Teller (BET) and Barrett–Joyner–Halenda (BJH) systems were used to calculate the specific surface area and pore size distributions. The energy dispersive X-ray spectroscopy (EDS) and scanning electron microscopy (SEM) analyses were conducted on a SU8010 scanning electron microscope (Tokyo, Japan) with a resolution of 10 kV. A JOEL 2100F (Tokyo, Japan) at 200 kV was used to obtain the transmission electron microscopy (TEM) images and EDS analysis was carried out with the instrument of Oxford X-MaxN 80 T IE250 (Oxford, UK). The ammonia temperature-programmed desorption analysis (NH₃-TPD) was performed on a BELCAT B instrument (Osaka, Japan). Fourier transform infrared spectra (FT-IR) were measured, making KBr pellets in an IS10 FTIR spectrometer (ThermoScientific, Waltham, MA, USA). The elemental analysis of the synthesized and recycled catalysts was conducted on a Perkin Elmer spectrometer OES Optima 5300 DV (Wellesley, MA, USA) through inductively coupled plasma optical emission spectroscopy (ICP-OES).

3.4. Activity and Product Analysis of Catalysts

The 5-HMF etherification was conducted in a microwave tube (20 mL) with a mixing of 1 mmol 5-HMF and 5 mL ethanol as a reactant and as a solvent in the microwave reactor of a monomodal CEM Discover SP. The reactions were conducted in various catalytic amounts, times, temperatures, and microwave powers. All the reactions were performed in triplicate and the mean deviation of the conversion and selectivity were in the range of ± 2 to 2.5. The internal temperature of the microwave was measured by an infrared sensor positioned underneath the microwave cavity. A small amount of the reaction solution was collected and quantitatively measured with gas chromatography linked with a mass spectrometer (GC-MS, Shimadzu QP2020, Kyoto, Japan) with a capillary column of SH-Rxi-5Sil MS (30 m 0.25 mm 0.25 m) at a predetermined period after the reaction had stopped. The program in the GC-MS was initially set to stable for 6 min at 40 °C and thereafter raised to 250 °C at 10 °C min⁻¹ rate with the flow of 1.1 mL min⁻¹. The MS detector temperature was 230 °C with the electron ionization mode of 70 eV. The interval 35–450 *m/z* was used to record the MS spectra. The NIST Mass spectral library was utilized to identify the individual compounds.

4. Conclusions

This research demonstrated the synthesis of a heterogeneous catalyst of encapsulated molybdophosphoric acid in KCC-1 for the microwave etherification of 5-HMF with ethanol. TEM and SEM morphological studies proved the encapsulation of molybdophosphoric acid with KCC-1. The encapsulation of molybdophosphoric acid during synthesis did not affect the materials' spherical morphology and formed uniform unimodal pores (12 nm). The MPA encapsulated catalyst promoted 82% 5-HMF conversion with a 12% and 82% selectivity of HMFDEA and EMFDEA at the optimum conditions. Even the IMPA-KCC-1 catalyst outperformed the MPA-KCC-1 catalyst in terms of catalytic activity but lost the metal sites during reactions, limiting its use as a heterogeneous catalyst. The catalytic activity of 5-HMF with ethanol in the presence of pure MPA formed more humin products due to its high acidity and also the separation of MPA from the reaction mixture would be a tedious process due to its homogeneous nature. It concluded that the encapsulation method builds a highly heterogeneous catalyst and also selectively forms an EMFDEA ether product. The encouraging results obtained in this study will open up new possibilities for the use of 5-HMF to fuel additive synthesis in the biorefinery process using an encapsulated molybdophosphoric acid KCC-1 catalyst.

Author Contributions: Conceptualization, S.V.V. and Q.B.; methodology, S.V.V.; software, S.V.V.; validation, S.V.V. and Q.B.; formal analysis, S.V.V., J.C. and Q.B.; investigation, S.V.V. and J.C.; resources, J.X., H.W., H.L. and Q.B.; data curation, S.V.V.; writing—original draft preparation, S.V.V. and Q.B.; writing—review and editing, S.V.V., J.X., H.W., H.L. and Q.B.; visualization, S.V.V. and J.C.; supervision, Q.B.; project administration, Q.B.; funding acquisition, J.X. and Q.B. All authors have read and agreed to the published version of the manuscript.

Funding: This research was funded by the National Natural Science Foundation of China (grant number 32171713), Jiangsu Agricultural Science and Technology Innovation Fund (grant number CX (22)3129), Jiangsu Province and Education Ministry Co-sponsored Synergistic Innovation Center of Modern Agricultural Equipment (grant number XTCX2012), and the Priority Academic Program Development of Jiangsu Higher Education Institutions (PAPD).

Data Availability Statement: The data that has been used is confidential.

Conflicts of Interest: The authors declare no conflict of interest.

References

1. Field, C.B.; Campbell, J.E.; Lobell, D.B. Biomass energy: The scale of the potential resource. *Trends Ecol. Evol.* **2008**, *23*, 65–72. [[CrossRef](#)] [[PubMed](#)]
2. Lam, H.L.; Varbanov, P.; Klemeš, J. Minimising carbon footprint of regional biomass supply chains. *Resour. Conserv. Recycl.* **2010**, *54*, 303–309. [[CrossRef](#)]

3. Nie, Y.; Li, J.; Wang, C.; Huang, G.; Fu, J.; Chang, S.; Li, H.; Ma, S.; Yu, L.; Cui, X.; et al. A fine-resolution estimation of the biomass resource potential across China from 2020 to 2100. *Resour. Conserv. Recycl.* **2022**, *176*, 105944. [[CrossRef](#)]
4. Opia, A.C.; Hamid, M.K.B.A.; Syahrullail, S.; Rahim, A.B.A.; Johnson, C.A.N. Biomass as a potential source of sustainable fuel, chemical and tribological materials—Overview. *Mater. Today Proc.* **2021**, *39*, 922–928. [[CrossRef](#)]
5. Mittal, A.; Pilath, H.M.; Johnson, D.K. Direct Conversion of Biomass Carbohydrates to Platform Chemicals: 5-Hydroxymethylfurfural (HMF) and Furfural. *Energy Fuels* **2020**, *34*, 3284–3293. [[CrossRef](#)]
6. Serrano-Ruiz, J.C.; West, R.M.; Dumesic, J.A. Catalytic Conversion of Renewable Biomass Resources to Fuels and Chemicals. *Annu. Rev. Chem. Biomol. Eng.* **2010**, *1*, 79–100. [[CrossRef](#)]
7. Tang, Z.-E.; Lim, S.; Pang, Y.-L.; Ong, H.-C.; Lee, K.-T. Synthesis of biomass as heterogeneous catalyst for application in biodiesel production: State of the art and fundamental review. *Renew. Sustain. Energy Rev.* **2018**, *92*, 235–253. [[CrossRef](#)]
8. Kong, X.; Zhu, Y.; Fang, Z.; Kozinski, J.A.; Butler, I.S.; Xu, L.; Song, H.; Wei, X. Catalytic conversion of 5-hydroxymethylfurfural to some value-added derivatives. *Green Chem.* **2018**, *20*, 3657–3682. [[CrossRef](#)]
9. Xu, C.; Paone, E.; Rodríguez-Padrón, D.; Luque, R.; Mauriello, F. Recent catalytic routes for the preparation and the upgrading of biomass derived furfural and 5-hydroxymethylfurfural. *Chem. Soc. Rev.* **2020**, *49*, 4273–4306. [[CrossRef](#)]
10. Zhao, Y.; Lu, K.; Xu, H.; Zhu, L.; Wang, S. A critical review of recent advances in the production of furfural and 5-hydroxymethylfurfural from lignocellulosic biomass through homogeneous catalytic hydrothermal conversion. *Renew. Sustain. Energy Rev.* **2021**, *139*, 110706. [[CrossRef](#)]
11. Alipour, S.; Omidvarborna, H.; Kim, D.-S. A review on synthesis of alkoxy methyl furfural, a biofuel candidate. *Renew. Sustain. Energy Rev.* **2017**, *71*, 908–926. [[CrossRef](#)]
12. Fan, W.; Verrier, C.; Queneau, Y.; Popowycz, F. 5-Hydroxymethylfurfural (HMF) in Organic Synthesis: A Review of its Recent Applications Towards Fine Chemicals. *Curr. Org. Synth.* **2019**, *16*, 583–614. [[CrossRef](#)]
13. Arias, K.S.; Climent, M.J.; Corma, A.; Iborra, S. Biomass-Derived Chemicals: Synthesis of Biodegradable Surfactant Ether Molecules from Hydroxymethylfurfural. *ChemSusChem* **2014**, *7*, 210–220. [[CrossRef](#)]
14. Sacia, E.R.; Balakrishnan, M.; Bell, A.T. Biomass conversion to diesel via the etherification of furanyl alcohols catalyzed by Amberlyst-15. *J. Catal.* **2014**, *313*, 70–79. [[CrossRef](#)]
15. Li, X.; Zhang, L.; Wang, S.; Wu, Y. Recent Advances in Aqueous-Phase Catalytic Conversions of Biomass Platform Chemicals Over Heterogeneous Catalysts. *Front. Chem.* **2020**, *7*, 948. [[CrossRef](#)]
16. Lanzafame, P.; Temi, D.M.; Perathoner, S.; Centi, G.; Macario, A.; Aloise, A.; Giordano, G.J.C.T. Etherification of 5-hydroxymethyl-2-furfural (HMF) with ethanol to biodiesel components using mesoporous solid acidic catalysts. *Catal. Today* **2011**, *175*, 435–441. [[CrossRef](#)]
17. Allen, M.C.; Hoffman, A.J.; Liu, T.-w.; Webber, M.S.; Hibbitts, D.; Schwartz, T.J. Highly Selective Cross-Etherification of 5-Hydroxymethylfurfural with Ethanol. *ACS Catal.* **2020**, *10*, 6771–6785. [[CrossRef](#)]
18. Isaeva, V.I.; Nefedov, O.M.; Kustov, L.M. Metal–Organic Frameworks-Based Catalysts for Biomass Processing. *Catalysts* **2018**, *8*, 368. [[CrossRef](#)]
19. Qiu, G.; Wang, X.; Huang, C.; Li, Y.; Chen, B. Facile, One-Pot, Two-Step, Strategy for the Production of Potential Bio-Diesel Candidates from Fructose. *Catalysts* **2017**, *7*, 237. [[CrossRef](#)]
20. Ayashi, N.; Najafi Chermahini, A.; Saraji, M. Biomass conversion to alkyl levulinates using heteropoly acid carbon mesoporous composites. *Process Saf. Environ. Prot.* **2022**, *160*, 988–1000. [[CrossRef](#)]
21. Afshari, M.; Varma, R.S.; Saghanezhad, S.J. Catalytic Applications of Heteropoly acid-Supported Nanomaterials in Synthetic Transformations and Environmental Remediation. *Comments Inorg. Chem.* **2022**, *43*, 129–176. [[CrossRef](#)]
22. Boahene, P.E.; Vedachalam, S.; Dalai, A.K. Catalytic oxidative desulfurization of light gas oil over Keggin-type phosphomolybdic acid supported on TUD-1 metallosilicates. *Fuel* **2022**, *317*, 123447. [[CrossRef](#)]
23. Chhabra, T.; Rohilla, J.; Krishnan, V. Nanoarchitectonics of phosphomolybdic acid supported on activated charcoal for selective conversion of furfuryl alcohol and levulinic acid to alkyl levulinates. *Mol. Catal.* **2022**, *519*, 112135. [[CrossRef](#)]
24. Zhou, S.; He, J.; Wu, P.; He, L.; Tao, D.; Lu, L.; Yu, Z.; Zhu, L.; Chao, Y.; Zhu, W. Metal-organic framework encapsulated high-loaded phosphomolybdic acid: A highly stable catalyst for oxidative desulfurization of 4,6-dimethyldibenzothiophene. *Fuel* **2022**, *309*, 122143. [[CrossRef](#)]
25. Winoto, H.P.; Fikri, Z.A.; Ha, J.-M.; Park, Y.-K.; Lee, H.; Suh, D.J.; Jae, J. Heteropolyacid supported on Zr-Beta zeolite as an active catalyst for one-pot transformation of furfural to γ -valerolactone. *Appl. Catal. B Environ.* **2019**, *241*, 588–597. [[CrossRef](#)]
26. Brahmkhatri, V.; Patel, A. Esterification of lauric acid with butanol-1 over H3PW12O40 supported on MCM-41. *Fuel* **2012**, *102*, 72–77. [[CrossRef](#)]
27. Alcañiz-Monge, J.; Bakkali, B.E.; Trautwein, G.; Reinoso, S. Zirconia-supported tungstophosphoric heteropolyacid as heterogeneous acid catalyst for biodiesel production. *Appl. Catal. B Environ.* **2018**, *224*, 194–203. [[CrossRef](#)]
28. Almeida, R.P.d.; Gomes Aciole, R.C.; Infantes-Molina, A.; Rodríguez-Castellón, E.; Andrade Pacheco, J.G.; Lopes Barros, I.d.C. Residue-based activated carbon from passion fruit seed as support to H3PW12O40 for the esterification of oleic acid. *J. Clean. Prod.* **2021**, *282*, 124477. [[CrossRef](#)]
29. Linares, N.; Silvestre-Albero, A.M.; Serrano, E.; Silvestre-Albero, J.; García-Martínez, J. Mesoporous materials for clean energy technologies. *Chem. Soc. Rev.* **2014**, *43*, 7681–7717. [[CrossRef](#)]

30. Cerón-Camacho, R.; Aburto, J.A.; Montiel, L.E.; Martínez-Palou, R. Microwave-assisted organic synthesis versus conventional heating. A comparative study for Fisher glycosidation of monosaccharides. *Comptes Rendus Chim.* **2013**, *16*, 427–432. [[CrossRef](#)]
31. Remón, J.; Randall, J.; Budarin, V.L.; Clark, J.H. Production of bio-fuels and chemicals by microwave-assisted, catalytic, hydrothermal liquefaction (MAC-HTL) of a mixture of pine and spruce biomass. *Green Chem.* **2019**, *21*, 284–299. [[CrossRef](#)]
32. Vasudevan, S.V.; Kong, X.; Cao, M.; Wang, M.; Mao, H.; Bu, Q. Microwave-assisted liquefaction of carbohydrates for 5-hydroxymethylfurfural using tungstophosphoric acid encapsulated dendritic fibrous mesoporous silica as a catalyst. *Sci. Total Environ.* **2021**, *760*, 143379. [[CrossRef](#)]
33. Sudhakar, P.; Pandurangan, A. Heteropolyacid (H3PW12O40)-impregnated mesoporous KIT-6 catalyst for green synthesis of bio-diesel using transesterification of non-edible neem oil. *Mater. Renew. Sustain. Energy* **2019**, *8*, 22. [[CrossRef](#)]
34. Ishikawa, S.; Ikeda, T.; Koutani, M.; Yasumura, S.; Amakawa, K.; Shimoda, K.; Jing, Y.; Toyao, T.; Sadakane, M.; Shimizu, K.-I.; et al. Oxidation Catalysis over Solid-State Keggin-Type Phosphomolybdic Acid with Oxygen Defects. *J. Am. Chem. Soc.* **2022**, *144*, 7693–7708. [[CrossRef](#)]
35. Vilanculo, C.B.; da Silva, M.J.; Rodrigues, A.A.; Ferreira, S.O.; da Silva, R.C. Vanadium-doped sodium phosphomolybdate salts as catalysts in the terpene alcohols oxidation with hydrogen peroxide. *RSC Adv.* **2021**, *11*, 24072–24085. [[CrossRef](#)]
36. Huang, X.; Tao, Z.; Praskavich, J.C.; Goswami, A.; Al-Sharab, J.F.; Minko, T.; Polshettiwar, V.; Asefa, T. Dendritic Silica Nanomaterials (KCC-1) with Fibrous Pore Structure Possess High DNA Adsorption Capacity and Effectively Deliver Genes In Vitro. *Langmuir* **2014**, *30*, 10886–10898. [[CrossRef](#)]
37. Tonutti, L.G.; Dalla Costa, B.O.; Mendow, G.; Pestana, G.L.; Veizaga, N.S.; Grau, J.M. Etherification of hydroxymethylfurfural with ethanol on mesoporous silica catalysts of regulated acidity to obtain ethoxymethylfurfural, a bio-additive for diesel. *Microporous Mesoporous Mater.* **2022**, *343*, 112145. [[CrossRef](#)]
38. Guo, H.; Dowaki, T.; Shen, F.; Qi, X.; Smith, R.L. Critical Assessment of Reaction Pathways for Next-Generation Biofuels from Renewable Resources: 5-Ethoxymethylfurfural. *ACS Sustain. Chem. Eng.* **2022**, *10*, 9002–9021. [[CrossRef](#)]

Disclaimer/Publisher's Note: The statements, opinions and data contained in all publications are solely those of the individual author(s) and contributor(s) and not of MDPI and/or the editor(s). MDPI and/or the editor(s) disclaim responsibility for any injury to people or property resulting from any ideas, methods, instructions or products referred to in the content.